


 Cite this: *RSC Adv.*, 2021, **11**, 15835

# Resin-supported iridium complex for low-temperature vanillin hydrogenation using formic acid in water†

 Christene A. Smith,<sup>‡</sup> Francesco Brandi,<sup>‡</sup>  Majd Al-Naji \* and Ryan Guterman \*

Biorefinery seeks to utilize biomass waste streams as a source of chemical precursors with which to feed the chemical industry. This goal seeks to replace petroleum as the main feedstock, however this task requires the development of efficient catalysts capable of transforming substances derived from biomass into useful chemical products. In this study, we demonstrate that a highly-active iridium complex can be solid-supported and used as a low-temperature catalyst for both the decomposition of formic acid (FA) to produce hydrogen, and as a hydrogenation catalyst to produce vanillyl alcohol (VA) and 2-methoxy-4-methylphenol (MMP) from vanillin (V); a lignin-derived feedstock. These hydrogenation products are promising precursors for epoxy resins and thus demonstrate an approach for their production without the need for petroleum. In contrast to other catalysts that require temperatures exceeding 100 °C, here we accomplish this at a temperature of <50 °C in water under autogenous pressure. This approach provides an avenue towards biorefinery with lower energy demands, which is central to the decentralization and broad implementation. We found that the high activity of the iridium complex transfers to the solid-support and is capable of accelerating the rate determining step; the decomposition of FA into hydrogen and carbon dioxide. The yield of both VA and MMP can be independently tuned depending on the temperature. The simplicity of this approach expands the utility of molecular metal complexes and provides new catalyst opportunities in biorefinery.

 Received 23rd February 2021  
 Accepted 14th April 2021

DOI: 10.1039/d1ra01460a

[rsc.li/rsc-advances](http://rsc.li/rsc-advances)

## Introduction

Catalysis is useful for a variety of transformations to synthesize pharmaceuticals and other value-added chemicals. Traditionally, metal complexes are used in catalysis because they are easily studied and modified to increase reactivity. One salient problem with them is their removal, which requires additional steps, solvent, and columns, nullifying the benefits of lower heat and time that they provide. Heterogeneous catalysts do not have the advantage of obtaining mechanistic insight and undergoing optimization to the degree of homogeneous catalysts, but they are easily removed from solution and do not require the intense work up procedures, unlike homogeneous catalysts. They also have the advantage of recyclability, which is crucial on an industrial scale for both environmental and economic reasons. Immobilization of known molecular catalysts onto a solid support harnesses the benefits of both homogeneous and heterogeneous catalysts with rational design and ease of removal. Recyclability with homogeneous catalysts

is possible, but the process is often costly and time consuming. Immobilization of molecular catalysts with known high activity on solid supports makes their recyclability accessible in industry and is one strategy to overcome their troublesome recovery. The potential of catalysis is often limited by the scale up necessary for industrial application and this is particularly the case in biorefinery,<sup>1–5</sup> which is an approach geared towards upgrading lignocellulosic biomass to valued-added chemicals in the so-called biorefinery processing.<sup>3,6</sup> Within this process, lignocellulosic biomass undergoes physico-chemicals transformation toward low-carbon footprint fine products.<sup>7</sup> Among these reactions, catalytic hydrogenation is a key reaction which allows the production of a wide range of compounds.<sup>8–10</sup> Typically, a biomass heterogeneously-catalyzed hydrogenation reaction is conducted using relatively high temperature (100–200 °C), external pressurized H<sub>2</sub> as reductive agent and supported metals as catalyst, such as Pt, Pd, Ru and Ni.<sup>8,9,11–14</sup> Heterogeneous catalysis is the preferred method because it allows for the implementation of more economically efficient and environmentally benign reactor designs. However, biorefinery processes are expensive when compared to traditional refineries. In fact, the complexity of lignocellulosic biomass requires a large number of cost-effective processing steps. Reducing the reaction temperature and pressure using new catalysts,<sup>2</sup> replacing H<sub>2</sub> with formic acid (FA),<sup>14–18</sup> and achieving

Department of Colloid Chemistry, Max Planck Institute of Colloids and Interfaces, Am Mühlenberg 1, 14476 Potsdam, Germany. E-mail: [Ryan.guterman@mpikg.mpg.de](mailto:Ryan.guterman@mpikg.mpg.de)

† Electronic supplementary information (ESI) available. See DOI: 10.1039/d1ra01460a

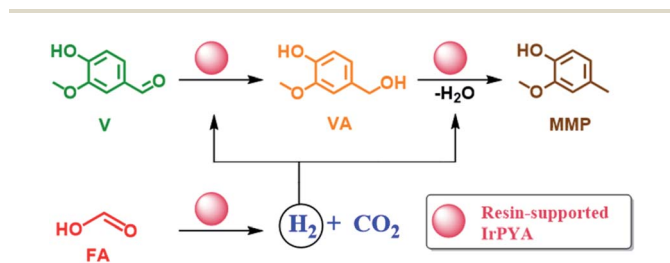
‡ These authors contributed equally to the manuscript.



this using solid-supported catalysts are three viable strategies to reduce the cost of biorefinery. Innate difficulties in transporting and storing  $H_2$  poses a significant hurdle to biorefinery, where hydrogenation reactions are invariably needed to convert oxygen-rich biomaterial into useful substances for the chemical industry. Formic acid has emerged as a solution<sup>19</sup> since it can be easily stored as a liquid and can be produced at low temperature from  $CO_2$  and  $H_2$  or by biomass processing.<sup>20</sup> Furthermore, current efforts to efficiently produce formic acid seeks to bolster the “formic acid economy” as a pillar for future endeavours in green energy and biorefinery.<sup>21</sup> Formic acid decomposition to hydrogen needs the assistance of a strong catalyst in order to lower the overall temperature of the reaction. Ru and Ir molecular catalysts are among the most commonly used for this purpose a wide variety of structures producing different dehydrogenation capabilities with dehydrogenation occurring at low temperature in many cases.<sup>22</sup> Iridium is known to be active in this reaction as known by Himeda.<sup>23</sup> It is also known to be an efficient hydrogenation catalyst of carbonyls as shown by Albrecht and co-workers.<sup>24</sup> Therefore it is an ideal catalyst not just to convert formic acid to hydrogen, but to also convert a potential lignin feedstock to various other value-added chemicals at low temperature.

Vanillin (**V**) is nowadays the major lignin-derived feedstock already produced in industrial scale, mostly by Borregaard company.<sup>25,26</sup> Vanillin itself is already used as a flavor in the food and cosmetic industry.<sup>27</sup> Vanillin has the potential to be upgraded to value-added compounds *via* catalytic hydrogenation. Indeed, the hydrogenation products of vanillin, *i.e.* Vanillyl alcohol (**VA**) and 2-methoxy-4-methylphenol (**MMP**), can be used respectively, as flavor and bio-fuel, while both are promising precursors of sustainable epoxy resins.<sup>8,28,29</sup>

Vanillin hydrogenation proceeds toward **VA** and then presents a hydrodeoxygenation step to **MMP**, *viz.* in Scheme 1. To date, several studies have studied **V** hydrogenation, using supported metal catalysts (Pd, Ru, Rh, Pd, Au, Pt and Ni) under pressurized  $H_2$ .<sup>8,30–33</sup> For example, Bindwal *et al.* reported **VA** and **MMP** yield of 90 mol% and 10 mol% respectively, at 65 °C with Ru/C and 2.1 MPa of  $H_2$ .<sup>33</sup> Similarly, we recently reported on a complete conversion of **V** to **MMP** at 150 °C and 2.5 MPa using Ni supported on nitrogen doped carbon catalysts in a continuous flow system.<sup>8</sup> As it can be seen, most reported studies of **V** hydrogenation reported a high **V** conversion and **VA** and **MMP** yields but at relatively high temperatures (60–150 °C)



Scheme 1 Hydrogenation of vanillin (**V**) to vanillyl alcohol (**VA**) and subsequently to 4-methyl-2-methoxyphenol (**MMP**) using formic acid as a reducing agent over IrPYA resin catalyst.

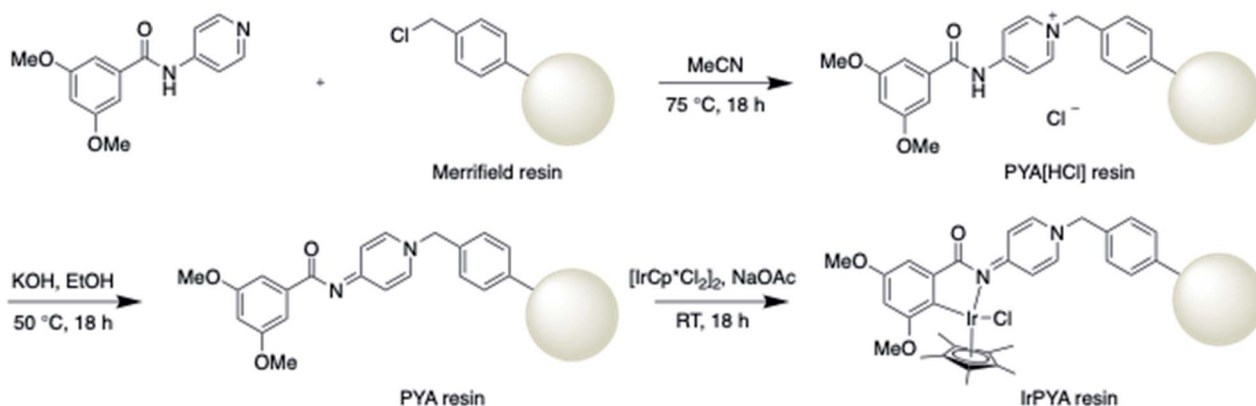
and  $H_2$  pressure (2–2.5 MPa). However, the utilization of alternative and sustainable hydrogen sources *e.g.*, **FA**, and the performance of **V** hydrogenation at room temperature was scarcely reported.<sup>14,34,35</sup> For biorefinery in particular, low-temperature and low-pressure methods offer reduced net energy demand, more simplistic setups and finally the need to centralize the biorefinery process in order to make the heat requirements economically feasible. At the moment, biorefinery centralization is required in order to reduce net energy demands by recycling heat, however low-temperature approaches allows for decentralization and thus reduces transportation costs for raw materials. For example, a study examining the cost of straw valorization in Baden-Wuerttemberg, Germany, found that a centralized biorefinery approach results in a transportation cost of 10% of the total cost for straw.<sup>36</sup> Furthermore, they explained that smaller, decentralized biorefineries offer better price-to-quantity ratios and are less sensitive to feedstock cost fluctuations. This is in contrast to larger biorefineries that require a constant supply of larger volumes of low-cost material and thus become less profitable when feedstock value increase in price. For these reasons, efforts towards smaller, decentralized biorefineries *via* lower heating requirements and simpler setups can improve the profitability of biorefinery.

In this context, we report the use of a solid-supported iridium complex as a low-temperature catalyst for **V** upgrading using **FA**. Utilizing a molecular complex provides the benefit of harnessing developed methodologies for homogenous catalysts, but with the convenience of a heterogeneous catalyst for separation. The resin supported Ir catalyst (**IrPYA**) was able to decompose **FA** into hydrogen at low temperature (50 °C), with maximum **FA** conversion of 76 mol%. The supported iridium catalyst was also found to be active for **V** hydrogenation toward **VA** and **MMP** in the presence of **FA** as a hydrogen source. Product selectivity was found tunable with temperature, yielding a maximum of 54 mol% of **VA** at 25 °C and a maximum of 24 mol% of **MMP** at 50 °C. These results demonstrate how metal complexes may be harnessed on solid-supports and their use expanded in low-temperature and low-pressure biorefinery.

## Results and discussion

### IrPYA resin synthesis

First 3,5-dimethoxy-*N*-(pyridin-4-yl)benzamide was reacted with Merrifield resin in acetonitrile at 75 °C for 18 hours (Scheme 2). After the reaction, the resin was washed several times with hot acetonitrile to remove any precursor and then dried to give **PYA [HCl] resin**. Reaction completion was observed by FTIR (Fig. S1 in the ESI<sup>†</sup>). Then an altered procedure for proton removal was done by reacting the **PYA [HCl] resin** in a solution of KOH in EtOH at 50 °C overnight to give the **PYA resin** (Scheme 2). The resin was washed with hot EtOH and then  $H_2O$  to remove any KOH. The material was then washed with acetone to remove any  $H_2O$  and then dried in a vacuum oven. The prepared ligand resin (**PYA resin**) was observed by FTIR (Fig. S2 in the ESI<sup>†</sup>). Then metalation of the supported ligand was done by reacting the **PYA resin** with  $[IrCp^*Cl_2]_2$  and NaOAc in dichloromethane at room temperature for 18 hours (Scheme 2). The material was then washed with dichloromethane,  $H_2O$ , and acetone before drying. The final



Scheme 2 Synthesis of the IrPYA resin.

supported catalyst material **IrPYA resin** was confirmed by FTIR (Fig. S3 in the ESI<sup>†</sup>). In all cases FTIR was compared with a molecular species for confirmation of reaction completion (Fig. S1–S3 in the ESI<sup>†</sup>) and in the case of the metalation reaction XPS analysis was also performed on both the molecular and supported catalyst for additional confirmation (Fig. 1).

The XPS spectra of the **IrPYA resin** material matched with that of the homogeneous **IrPYA complex**, showing a single oxidation state (Fig. 1). The **IrPYA resin** has a  $4f_{5/2}$  peak at 64.8 eV and the  $4f_{7/2}$  peak at 61.8 eV (red, Fig. 1), and the **IrPYA complex** shows a  $4f_{5/2}$  peak at 64.8 eV and a  $4f_{7/2}$  peak at 61.7 eV (black, Fig. 1). This shows that the synthesized material contains a molecular catalyst and no nanoparticle formation is observed on the surface of the resin.

### Catalyst evaluation

An iridium complex was successfully supported on Merrifield resin and used as a catalyst for the simultaneous decomposition of **FA** and production of **VA** and **MMP** from **V**. The activity of the

synthesized **IrPYA resin** catalyst in the hydrogenation of **V** to **VA** and the subsequent product **MMP** was studied using **FA** as a reducing agent in the presence of **KOH** (Scheme 1). The performance of the catalyst was initially investigated at room temperature (25 °C), with samples collected at different reaction times (after 1 h, 2.5 h and 5 h), *viz.* in Fig. 2. After 1 h, the conversion of **V** was 99 mol% with a **VA** and **MMP** yield of 69 mol% and 5.2 mol% respectively. This demonstrates that a single catalyst can both dehydrogenate **FA** and hydrogenate **V** and **VA** within a reaction vessel. The solution after the reaction remained colourless, indicating that the strongly coloured metal center remained bound to the resin. Increasing the reaction time from 1 h to 2.5 h did not result in a significant increase of  $Y_{VA}$  (from 69 mol% to 70 mol%) and  $Y_{MMP}$  (from 5.2 mol% to 5.8 mol%), *cf.* Fig. 2. To correlate catalyst performance in **V** hydrogenation to **FA** decomposition towards  $H_2$  and  $CO_2$ , a separate experiment was conducted to investigate the **FA** degradation rate in absence of **V**, *cf.* Fig. S6 at ESI<sup>†</sup>. In this case, **FA** conversion, increases from 6.7 mol% to 15.7 mol% after 2.5 h, *cf.* Fig. S6 in ESI<sup>†</sup>. These results combined with the insignificant change in **V** conversion between 1 and 2.5 h

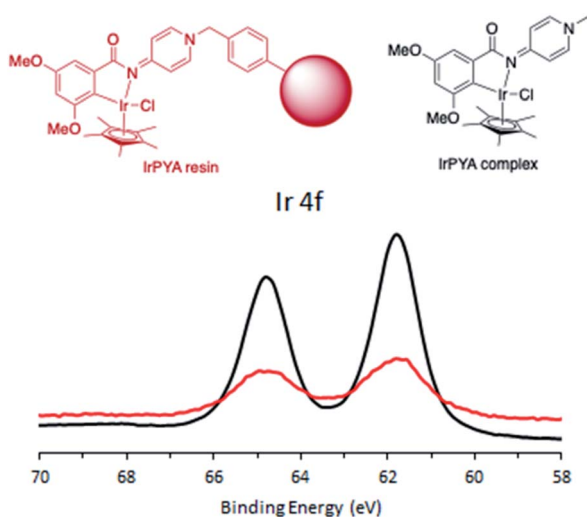


Fig. 1 Ir 4f region of the XPS spectra of the IrPYA resin (red) and the IrPYA complex (black).

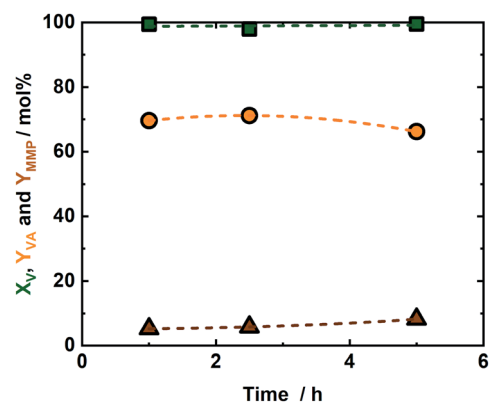


Fig. 2 The conversion of vanillin ( $X_V$ ) and the yield of vanillyl alcohol and 4-methyl-2-methoxyphenol ( $Y_{VA}$  and  $Y_{MMP}$ ) as a function of the reaction time; reaction conditions:  $c_V = (715 \mu\text{L}, 1 \text{ wt}\%, 0.047 \text{ mmol})$ ,  $c_{FA} = (293 \mu\text{L}, 7.78 \text{ mmol})$ ,  $c_{KOH} (515 \mu\text{L}, 2 \text{ M}, 1.03 \text{ mmol})$ ,  $T = 25 \text{ }^\circ\text{C}$  and autogenous pressure ( $<1.0 \text{ MPa}$ ).

indicates that the Ir active sites are occupied firstly by **FA**. A further extension of the reaction time to 5 h resulted in an increase of  $Y_{\text{MMP}}$  from 5.8 mol% to 8.2 mol% combined with reduction of  $Y_{\text{VA}}$  from 71 mol% to 66 mol% as a result of its conversion to **MMP**. This increase of **MMP** yield is correlated to the increase in **FA** conversion from 15.7 mol% to 21 mol%, which liberated the active Ir sites to **V** that undergoes to hydrogenation reaction (Fig. S6†). This observation indicates that the decomposition of **FA** to  $\text{H}_2$  and  $\text{CO}_2$  is the rate determining step for the hydrogenation of **VA** to **MMP** and is in-line with our previous studies for hydrogenation of levulinic acid and **V** as a model mixture,<sup>14</sup> as well as  $\gamma$ -valerolactone hydrogenation to pentanoic acid using formic acid as a reducing agent.<sup>14</sup> Moreover, the 21 mol% conversion of **FA** at room temperature is a comparable value to similar studies conducted with homogeneous Ir-catalyst,<sup>37</sup> but here obtained with immobilized **IrPYA** which can potentially open new application in the field of heterogeneous catalysis and fuel cells.<sup>38–40</sup> As this catalyst uniquely contains the **IrPYA** supported on Merrifield resin (the catalyst is in solid form) and the **IrPYA** not used as homogenous catalyst, as well as the reaction conditions is mild ( $T = 50\text{ }^\circ\text{C}$  and autogenous pressure), we anticipate that no difference in the catalytic performance should be observed. In addition, research on this issue coupled with advanced characterization techniques are ongoing at our laboratory to further understand the unique performance and its potential scalability.

In order to maximize the  $Y_{\text{MMP}}$  the reaction temperature was increased from  $25\text{ }^\circ\text{C}$  to  $35\text{ }^\circ\text{C}$  and subsequently to  $50\text{ }^\circ\text{C}$  (Fig. S6–S8 in the ESI†). The experiment conducted at  $35\text{ }^\circ\text{C}$  resulted in only slight improvement of  $Y_{\text{MMP}}$  when compared to the  $25\text{ }^\circ\text{C}$  experiment (Fig. 3 and S9 in the ESI†). A further increase in reaction temperature to  $50\text{ }^\circ\text{C}$ , reduced  $Y_{\text{VA}}$  from 54 mol% to 44 mol% and increased  $Y_{\text{MMP}}$  from 8 mol% to 24 mol%, cf. Fig. 3 and S8 in the ESI†. This high  $Y_{\text{MMP}}$  is correlated to the high  $X_{\text{FA}}$  (76 mol%) at  $50\text{ }^\circ\text{C}$  after 5 h of reaction time (Fig. 3), which leads to a higher availability of active sites with respect to the experiments at  $25\text{ }^\circ\text{C}$  and  $35\text{ }^\circ\text{C}$ . Finally and noteworthy to be mentioned, the mass balance loss of

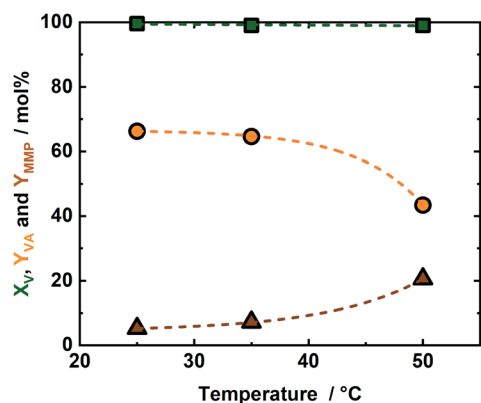


Fig. 3 The conversion of vanillin ( $X_{\text{V}}$ ) and the yield of vanillyl alcohol and 4-methyl-2-methoxyphenol ( $Y_{\text{VA}}$  and  $Y_{\text{MMP}}$ ) as a function of the reaction temperature; reaction conditions:  $c_{\text{V}} = (715\ \mu\text{L}, 1\ \text{wt}\%, 0.047\ \text{mmol})$ ,  $c_{\text{FA}} = (293\ \mu\text{L}, 7.78\ \text{mmol})$ ,  $c_{\text{KOH}} (515\ \mu\text{L}, 2\ \text{M}, 1.03\ \text{mmol})$ , reaction = 5 h and autogenous pressure ( $<1.0\ \text{MPa}$ ).

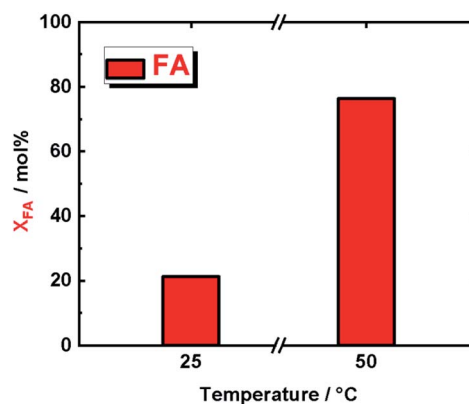


Fig. 4 A comparison in the conversion of formic acid ( $X_{\text{FA}}$ ) at  $25\text{ }^\circ\text{C}$  and  $50\text{ }^\circ\text{C}$  after 5 h of reaction time; reaction conditions:  $c_{\text{FA}} = (293\ \mu\text{L}, 7.78\ \text{mmol})$ ,  $c_{\text{KOH}} (515\ \mu\text{L}, 2\ \text{M}, 1.03\ \text{mmol})$ , and autogenous pressure ( $<1.0\ \text{MPa}$ ).

$\sim 23\text{ mol}\%$  is attributed to deposition of the **VA** and **MMP** on the surface of the catalyst due to its low solubility in water.<sup>41</sup> This  $Y_{\text{MMP}}$  is relatively low if compared to a similar study conducted at same temperature with pressurized  $\text{H}_2$  as the hydrogen source or with **FA** as the hydrogen source but at higher temperature, but is based using milder condition.<sup>14,35</sup> Moreover, the selectivity toward **VA** or **MMP** can be tuned according to temperature.

In order to confirm that our supported molecular catalyst, **IrPYA resin**, was indeed decomposing formic acid we subjected it to the same reaction conditions as in the **V** to **VA** and **MMP** reactions at both  $25\text{ }^\circ\text{C}$  and  $50\text{ }^\circ\text{C}$  (Fig. 4). At  $25\text{ }^\circ\text{C}$  we observed a decomposition  $X_{\text{FA}}$  of 21% and at  $50\text{ }^\circ\text{C}$  a  $X_{\text{FA}}$  of 76%. Although the conversion of formic acid at room temperature is approximately a third of its conversion at  $50\text{ }^\circ\text{C}$ , this still provides an excess of hydrogen for the conversion of **V** to **VA** and **MMP** in our reaction, as we used a large excess. Moreover, the **FA** decomposition at this lower temperatures, *i.e.*  $25\text{ }^\circ\text{C}$  and  $50\text{ }^\circ\text{C}$ , is typical of Ir complexes used as homogeneous catalysts.<sup>22</sup> This finding confirm that immobilized **IrPYA** has the same catalytic activity as homogenous Ir catalysts. Extending these findings in biorefinery will require flow reactors to be designed that take advantage of the dual behaviour of **IrPYA** supported on Merrifield resin. Using this catalyst in our previously reported continuous flow system for hydrogenation of vanillin will result in lower reaction temperature (from  $150\text{ }^\circ\text{C}$  to  $50\text{ }^\circ\text{C}$ ), as well as a reduction in system pressure from  $6.0\ \text{MPa}$  to below  $1.0\ \text{MPa}$ . All these will lead to efficient and selective process coupled with high economic efficiency biorefinery process (due to mild operating conditions). In addition, this type of hydrogenation with **IrPYA** supported on Merrifield resin can be expanded to wide range of biomass-derived compounds such as glucose, 5-hydroxymethylfurfural, levulinic acid and  $\gamma$ -valerolactone.

## Conclusions

An iridium complex was successfully supported on Merrifield resin and used as a catalyst for the simultaneous decomposition



of FA and production of VA and MMP from V. This approach harnesses the high activity and tunability of molecular metal complexes, but with the convenience and ease of separation of heterogeneous catalysts. Catalytic production of MMP typically takes place at temperatures exceeding 100 °C, however here it was accomplished at temperatures <50 °C. This was achieved by taking advantage of the high activity of the iridium complex, which is capable of accelerating the rate determining step; the decomposition of FA to H<sub>2</sub> and CO<sub>2</sub>. Once this occurs, hydrogenation of V and VA proceeds using the same iridium complex as an active hydrogenation catalyst. As well, the VA and MMP yield was found to be tunable with temperature, providing a convenient means to tune product formation. While iridium is an expensive metal, it promotes mild reaction conditions and thus helps to offset other costs including heating and equipment designed for high temperature and pressures. As well, we believe that as formic acid becomes more integrated into the green economy, its use in biorefinery as a hydrogen source will become more prevalent. These results provide new prospects for decentralized biorefinery *via* low energy demands and expands the Frontier for supported molecular metal complexes in biomass upgrading.

## Author contributions

Christene A. Smith and Francesco Brandi were the prime experimentalists. Ryan Guterman and Majd Al-Naji supervised the research.

## Conflicts of interest

There are no conflicts to declare.

## Acknowledgements

We thank the Max Planck Society for their ongoing support. We thank Ursula Lubahn for her assistance with data management, Antje Völkel for her assistance with FTIR measurements and Jessica Brandt for her assistance with ICP measurements. We thank Markus Antonietti for his fruitful discussions, ongoing support, wisdom, and his lead vocals. This work was funded by the Max Planck Society.

## Notes and references

- 1 A. Corma Canos, S. Iborra and A. Velty, *Chem. Rev.*, 2007, **107**, 2411–2502.
- 2 P. Anastas and N. Eghbali, *Chem. Soc. Rev.*, 2010, **39**, 301–312.
- 3 D. Esposito and M. Antonietti, *Chem. Soc. Rev.*, 2015, **44**, 5821–5835.
- 4 R. Guterman, V. Molinari and E. Josef, *Angew. Chem.*, 2019, **131**, 13178–13184.
- 5 J. A. Mendoza Mesa, F. Brandi, I. Shekova, M. Antonietti and M. Al-Naji, *Green Chem.*, 2020, **22**, 7398–7405.
- 6 M. Al-Naji, H. Schlaad and M. Antonietti, *Macromol. Rapid Commun.*, 2020, 2000485.
- 7 Y. Liao, S. F. Koelewijn, G. van den Bossche, J. van Aelst, S. van den Bosch, T. Renders, K. Navare, T. Nicolaï, K. van Aelst, M. Maesen, H. Matsushima, J. M. Thevelein, K. van Acker, B. Lagrain, D. Verboekend and B. F. Sels, *Science*, 2020, **367**, 1385–1390.
- 8 F. Brandi, M. Bäuml, V. Molinari, I. Shekova, I. Laueremann, T. Heil, M. Antonietti and M. Al-Naji, *Green Chem.*, 2020, **22**, 2755–2766.
- 9 M. Besson, P. Gallezot and C. Pinel, *Chem. Rev.*, 2014, **114**, 1827–1870.
- 10 M. J. Climent, A. Corma and S. Iborra, *Green Chem.*, 2014, **16**, 516–547.
- 11 F. Brandi, M. Bäuml, I. Shekova, V. Molinari and M. Al-Naji, *Sustainable Chem.*, 2020, **1**, 106–115.
- 12 M. Al-Naji, A. M. Balu, A. Roibu, M. Goepel, W. D. Einicke, R. Luque and R. Gläser, *Catal. Sci. Technol.*, 2015, **5**, 2085–2091.
- 13 S. Bailey and F. King, in *Fine Chemicals through Heterogeneous Catalysis*, Wiley-VCH Verlag GmbH, Weinheim, Germany, 2007, pp. 351–471.
- 14 M. Al-Naji, M. Popova, Z. Chen, N. Wilde and R. Gläser, *ACS Sustainable Chem. Eng.*, 2020, **8**, 393–402.
- 15 M. Al-Naji, J. Van Aelst, Y. Liao, M. D'Hullian, Z. Tian, C. Wang, R. Gläser and B. F. Sels, *Green Chem.*, 2020, **22**, 1171–1181.
- 16 M. J. Gilkey and B. Xu, *ACS Catal.*, 2016, **6**, 1420–1436.
- 17 S. De, B. Saha and R. Luque, *Bioresour. Technol.*, 2015, **178**, 108–118.
- 18 M. Al-Naji, A. Yopez, A. M. Balu, A. A. Romero, Z. Chen, N. Wilde, H. Li, K. Shih, R. Gläser and R. Luque, *J. Mol. Catal. A: Chem.*, 2016, **417**, 145–152.
- 19 R. van Putten, T. Wissink, T. Swinkels and E. A. Pidko, *Int. J. Hydrogen Energy*, 2019, **44**, 28533–28541.
- 20 M. Nielsen, E. Alberico, W. Baumann, H. J. Drexler, H. Junge, S. Gladiali and M. Beller, *Nature*, 2013, **495**, 85–89.
- 21 A. Weillhard, S. P. Argent and V. Sans, *Nat. Commun.*, 2021, **12**, 1–7.
- 22 J. H. Barnard, C. Wang, N. G. Berry and J. Xiao, *Chem. Sci.*, 2013, **4**, 1234–1244.
- 23 Y. Himeda, *Green Chem.*, 2009, **11**, 2018–2022.
- 24 M. Navarro, C. A. Smith and M. Albrecht, *Inorg. Chem.*, 2017, **56**, 11688–11701.
- 25 M. Fache, B. Boutevin and S. Caillol, *ACS Sustainable Chem. Eng.*, 2016, **4**, 35–46.
- 26 Borregaard, Smart Vanillin.
- 27 I. K. Ilic, M. Meurer, S. Chaleawert-Umpon, M. Antonietti and C. Liedel, *RSC Adv.*, 2019, **9**, 4591–4598.
- 28 F. Liguori, C. Moreno-Marrodan and P. Barbaro, *Chem. Soc. Rev.*, 2020, **49**, 6329–6363.
- 29 H. A. Meylemans, T. J. Groshens and B. G. Harvey, *ChemSusChem*, 2012, **5**, 206–210.
- 30 R. Nie, H. Yang, H. Zhang, X. Yu, X. Lu, D. Zhou and Q. Xia, *Green Chem.*, 2017, **19**, 3126–3134.
- 31 S. C. Shit, R. Singuru, S. Pollastri, B. Joseph, B. S. Rao, N. Lingaiah and J. Mondal, *Catal. Sci. Technol.*, 2018, **8**, 2195–2210.
- 32 J. L. Santos, M. Alda-Onggar, V. Fedorov, M. Peurla, K. Eränen, P. Mäki-Arvela, M. Centeno and D. Y. Murzin, *Appl. Catal., A*, 2018, **561**, 137–149.

- 33 A. B. Bindwal and P. D. Vaidya, *Energy Fuels*, 2014, **28**, 3357–3362.
- 34 B. Pongthawornsakun, P. Kaewsuanjik, P. Kittipreechakun, M. Ratova, P. Kelly, O. Mekasuwandumrong, P. Prasertdam and J. Panpranot, *Catal. Today*, 2020, **358**, 51–59.
- 35 P. Hao, D. K. Schwartz and J. W. Medlin, *Appl. Catal., A*, 2018, **561**, 1–6.
- 36 E. Petig, A. Rudi, E. Angenendt, F. Schultmann and E. Bahrs, *GCB Bioenergy*, 2019, **11**, 304–325.
- 37 S. M. Lu, Z. Wang, J. Wang, J. Li and C. Li, *Green Chem.*, 2018, **20**, 1835–1840.
- 38 C. Guan, Y. Pan, T. Zhang, M. J. Ajitha and K. Huang, *Chem.–Asian J.*, 2020, **15**, 937–946.
- 39 Y. Maenaka, T. Suenobu and S. Fukuzumi, *Energy Environ. Sci.*, 2012, **5**, 7360–7367.
- 40 J. Eppinger and K. W. Huang, *ACS Energy Lett.*, 2017, **2**, 188–195.
- 41 X. Yang, Y. Liang, X. Zhao, Y. Song, L. Hu, X. Wang, Z. Wang and J. Qiu, *RSC Adv.*, 2014, **4**, 31932–31936.